

## Article

# Highly Porous Carbons Synthesized from Tannic Acid via a Combined Mechanochemical Salt-Templating and Mild Activation Strategy

Sylwia Głowniak <sup>1</sup>, Barbara Szczęśniak <sup>1,\*</sup> , Jerzy Choma <sup>1</sup>  and Mietek Jaroniec <sup>2</sup> 

<sup>1</sup> Institute of Chemistry, Military University of Technology, 00-908 Warsaw, Poland; sylwia.glowniak@wat.edu.pl (S.G.); jerzy.choma@wat.edu.pl (J.C.)

<sup>2</sup> Department of Chemistry and Biochemistry, Advanced Materials and Liquid Crystal Institute, Kent State University, Kent, OH 44242, USA; jaroniec@kent.edu

\* Correspondence: barbara.szczesniak@wat.edu.pl; Tel.: +48-261-839-774

**Abstract:** Highly porous activated carbons were synthesized via the mechanochemical salt-templating method using both sustainable precursors and sustainable chemical activators. Tannic acid is a polyphenolic compound derived from biomass, which, together with urea, can serve as a low-cost, environmentally friendly precursor for the preparation of efficient N-doped carbons. The use of various organic and inorganic salts as activating agents afforded carbons with diverse structural and physicochemical characteristics, e.g., their specific surface areas ranged from 1190 m<sup>2</sup>·g<sup>-1</sup> to 3060 m<sup>2</sup>·g<sup>-1</sup>. Coupling the salt-templating method and chemical activation with potassium oxalate appeared to be an efficient strategy for the synthesis of a highly porous carbon with a specific surface area of 3060 m<sup>2</sup>·g<sup>-1</sup>, a large total pore volume of 3.07 cm<sup>3</sup>·g<sup>-1</sup> and high H<sub>2</sub> and CO<sub>2</sub> adsorption capacities of 13.2 mmol·g<sup>-1</sup> at −196 °C and 4.7 mmol·g<sup>-1</sup> at 0 °C, respectively. The most microporous carbon from the series exhibited a CO<sub>2</sub> uptake capacity as high as 6.4 mmol·g<sup>-1</sup> at 1 bar and 0 °C. Moreover, these samples showed exceptionally high thermal stability. Such activated carbons obtained from readily available sustainable precursors and activators are attractive for several applications in adsorption and catalysis.

**Keywords:** mechanochemistry; activated carbons; non-hazardous activators; salt-templating; ball milling



**Citation:** Głowniak, S.; Szczęśniak, B.; Choma, J.; Jaroniec, M. Highly Porous Carbons Synthesized from Tannic Acid via a Combined Mechanochemical Salt-Templating and Mild Activation Strategy.

*Molecules* **2021**, *26*, 1826. <https://doi.org/10.3390/molecules26071826>

Academic Editor: Marek Kosmowski

Received: 27 February 2021

Accepted: 22 March 2021

Published: 24 March 2021

**Publisher's Note:** MDPI stays neutral with regard to jurisdictional claims in published maps and institutional affiliations.



**Copyright:** © 2021 by the authors. Licensee MDPI, Basel, Switzerland. This article is an open access article distributed under the terms and conditions of the Creative Commons Attribution (CC BY) license (<https://creativecommons.org/licenses/by/4.0/>).

## 1. Introduction

Energy demand is now greater than ever, which results in significant fossil fuel consumption and related problems, e.g., excessive emissions of greenhouse gases. Recent research efforts have been directed toward the development of new green and efficient methods for energy conversion and storage as well as the reduction of anthropogenic gaseous emissions, which are responsible for global warming effects. Most of the proposed solutions are based on the usage of supercapacitors, fuel cells and batteries that exploit porous materials. For these uses, porous carbons have attracted particular interest due to their great adsorption properties resulting from high specific surface areas (SSAs), even above 3000 m<sup>2</sup>·g<sup>-1</sup>. Activated carbons have found widespread uses for diverse applications, e.g., water purification [1], gas adsorption [2] and energy storage [3]. The great merits of these materials include widely available precursors and the simplicity of preparation. Typically, the synthesis of activated carbons consists of two steps—carbonization, in which a carbon precursor undergoes pyrolysis in an inert atmosphere, and physical or chemical activation applied to develop porosity in the carbonized material. Physical activation usually involves heating a carbonaceous material under flowing air, steam or carbon dioxide, whereas chemical activation is conducted in the presence of activating agents, e.g., KOH, H<sub>3</sub>PO<sub>4</sub> and ZnCl<sub>2</sub>. Lately, an alternative salt-templating strategy has been proposed, in

which eutectic salts act as both templates and activators. This method afforded hierarchical carbons that featured good pore connectivity, assuring good mass transfer compared to solely microporous carbons [4,5]. For example, Pampel et al. [4] utilized a salt-templating method to obtain porous carbons by pyrolyzing a mixture of glucose and KCl/ZnCl<sub>2</sub>. Varying KCl content in the mixture resulted in activated carbons with tailored porosity and high SSA in the range of 960 to 2160 m<sup>2</sup>·g<sup>-1</sup>.

Solution-based methods for the synthesis of functional materials that rely on the use of solvents have prevailed at the laboratory and industrial scales. However, these methods are usually complex, time- and energy-consuming, and contribute to the accumulation of harmful waste solutions. Therefore, the mass production of functional materials should be adjusted to meet green chemistry requirements. A field containing great promise in terms of the more environmentally friendly synthesis of porous materials is mechanochemistry [6,7]. According to the IUPAC definition, a mechanochemical reaction is a chemical reaction that is induced by direct absorption of mechanical energy during shearing, stretching, grinding, etc. [8]. The beginnings of mechanochemistry date back to prehistoric times, when early people discovered the possibility of starting a fire by rubbing two stones together. Readers are referred to the excellent reviews devoted to the history of mechanochemistry [9,10]. Mechanochemistry has been implemented in metallurgy, pharmacy, catalysis and organic chemistry [11]. Although its utilization in the fabrication of porous materials is a rather new concept, it is an up-and-coming approach to overcoming the drawbacks of solution-based synthesis methods. Nowadays, mechanochemical reactions are usually carried out in automatic ball mills, where high energy milling is available. Typically, the generated mechanical energy is directly targeted to initiate chemical conversions on the surface of solid reactants; hence, additional heating is not needed. Mechanochemistry enables researchers to conduct reactions in solvent-free conditions (neat grinding, NG) or in the presence of small amounts of solvents (liquid-assisted grinding, LAG) [6]. Recent studies have indicated that mechanochemistry can be implemented for the preparation of highly porous carbon materials from sustainable precursors and non-hazardous activators [12–23]. For example, Schneidermann et al. [12] prepared N-doped carbons with high porosity from diverse wood components—lignin (SSA of 3199 m<sup>2</sup>·g<sup>-1</sup>), tannic acid (SSA of 2873 m<sup>2</sup>·g<sup>-1</sup>), wood waste (SSA of 2988 m<sup>2</sup>·g<sup>-1</sup>), cellulose (SSA of 1870 m<sup>2</sup>·g<sup>-1</sup>) and xylan (SSA of 1163 m<sup>2</sup>·g<sup>-1</sup>). The key step in the synthetic procedure involved one-step solvent-free ball milling of carbon precursor, urea used as a nitrogen source and K<sub>2</sub>CO<sub>3</sub> used as an activating agent. The as-prepared carbons exhibited a great performance as cathode materials for Li–S batteries with an initial discharge capacity up to 1300 mAh·g<sub>sulfur</sub><sup>-1</sup> (95% coulombic efficiency) and capacity retention above 75% within the first 50 cycles at a low electrolyte volume.

Theoretically, each carbon-rich material could be a precursor for activated carbons. However, to meet the demands of diverse applications, the selection of a proper precursor is very important. Biomass has shown great promise as a sustainable precursor for the preparation of functional carbons because it is a non-toxic, cheap, and renewable carbon source with carbon content even as high as 50%. Biomass employed for the preparation of activated carbons mainly originates from agriculture and forests, including dedicated crops, byproducts and residues. Producing porous carbons from biowastes is not only a cost-cutting strategy but is also a great solution for the utilization of an enormous number of presently useless products [1–3,24–31]. Tannins are a group of natural polyphenolic compounds extracted from various plants such as wood, fruit, bark, etc. Tannin-based extracts have already been used in various industrial sectors, e.g., as coagulants, adhesives, food additives and antioxidants [32,33]. Recently, natural tannin extracts have been proposed as efficient precursors for the synthesis of highly porous carbons [15,34–36] even with uniform and/or ordered porosity [5,21,37–40]. For example, Diez et al. [5] prepared carbons with SSA up to 2750 m<sup>2</sup>·g<sup>-1</sup> using tannic acid (TA) and K<sub>2</sub>CO<sub>3</sub>/KCl mixture as salts templates. Cai et al. [15] reported the mechanochemical synthesis of porous carbons with SSA up to 1800 m<sup>2</sup>·g<sup>-1</sup> from TA and FeCl<sub>3</sub>·6H<sub>2</sub>O. Elsewhere, implementing a salt-templating method,

Tiruye et al. [21] synthesized nitrogen-functionalized porous carbon nanospheres with TA and urea used as carbon precursors. The addition of an eutectic salt of  $\text{ZnCl}_2/\text{NaCl}$  during the synthesis led to activated carbons with SSAs up to  $1570 \text{ m}^2 \cdot \text{g}^{-1}$ . The eutectic salt mixture served as both the solvent and porogen in the synthesis. Non-carbonizable inorganic eutectic salts, which possess low melting points and are homogeneously miscible with carbon precursors, can effectively act as in situ pore forming agents, i.e., templates.

In this work, we present a green synthesis of highly porous carbons with SSAs up to  $3060 \text{ m}^2 \cdot \text{g}^{-1}$  using a one-pot ball milling method prior to the activation step. Mechanochemical reaction of TA—an eco-friendly biomass-derived carbon precursor—in the presence of non-hazardous organic and inorganic salts afforded highly porous carbons with great gas adsorption performance. Although there are many studies in the literature devoted to mechanochemical-assisted preparations of biomass-derived carbons using chemical activators or salt-templating methods, we did not find any paper in which both strategies using organic activators were implemented. Our approach combined two methods: salt-templating and mild chemical activation using organic or inorganic salts for the preparation of micro-mesoporous carbons. The low melting point of TA  $\sim 220 \text{ }^\circ\text{C}$ , makes it an appropriate substrate for this templating method based on the low melting point of the eutectic salt  $\text{NaCl}/\text{ZnCl}_2$ . Both tannic acid and the eutectic salt melt at around  $200 \text{ }^\circ\text{C}$ – $300 \text{ }^\circ\text{C}$ . At higher temperatures, the molten mixture undergoes carbonization and reacts with activating agents. In fact,  $\text{NaCl}$  acts as template, whereas  $\text{ZnCl}_2$  and the other added organic or inorganic salts, among oxalates, citrates and carbonates, support salt-templating until carbonization and then act as activating agents [4,5].

## 2. Results and Discussion

### 2.1. Morphological and Structural Characterization

A series of activated carbons was prepared from tannic acid and urea in the presence of the eutectic salt  $\text{NaCl}/\text{ZnCl}_2$ . The resulting carbons are denoted as C-ZN- $x$ , where ZN refers to the eutectic salt and  $x$  represents the activator used—pox (potassium oxalate,  $\text{K}_2\text{C}_2\text{O}_4$ ), aca (ammonium carbonate,  $(\text{NH}_4)_2\text{CO}_3$ ), pca (potassium carbonate,  $\text{K}_2\text{CO}_3$ ), pci (potassium citrate,  $\text{K}_3\text{C}_6\text{H}_5\text{O}_7$ ) or mci (magnesium citrate,  $\text{MgC}_6\text{H}_6\text{O}_7$ ). For instance, C-ZN-pox refers to the carbon sample obtained from tannic acid and urea with addition of the eutectic salt  $\text{NaCl}/\text{ZnCl}_2$  and potassium oxalate. Furthermore, C-pox was synthesized by the same method as C-ZN-pox, but without addition of ZN. Figure 1a shows the morphology of the selected samples, C-pox, C-ZN-pox and C-ZN. The activated carbon obtained from tannic acid and urea in the presence of the eutectic salt  $\text{NaCl}/\text{ZnCl}_2$ , i.e., C-ZN, is in the form of agglomerated spherical particles (Figure 1a(III,IV)). The morphologies of carbons activated with  $\text{K}_2\text{C}_2\text{O}_4$ , namely C-pox and C-ZN-pox, differ from that of C-ZN, revealing their highly porous structures (Figure 1a(I,II)). Elemental analysis of the selected samples provides information on their element contents (Table 1). Nitrogen content ranged from 1.01 to 5.94 wt.%, even though the amount of urea used in the syntheses of all samples remained the same. The lowest nitrogen content of 1.01 wt.% was determined for the C-pox sample prepared without the addition of the eutectic salt, indicating that the presence of  $\text{NaCl}$  and  $\text{ZnCl}_2$  inorganic salts was favorable for high nitrogen concentration in the resulting carbons. N contents of C-ZN and C-ZN-pox were 5.60 and 5.94 wt.%, respectively. It can be noted that using an additional activator (in this case, potassium oxalate) may contribute to the high N concentration in the activated carbons. Thermogravimetric analysis performed for these selected samples indicated their high thermal stability (Figure 1b). Total mass loss varied from 19.34% to 12.90% during heating up to  $900 \text{ }^\circ\text{C}$  in an inert atmosphere, including the mass drop at around  $100 \text{ }^\circ\text{C}$  associated with the evaporation of adsorbed water. In the temperature range  $300 \text{ }^\circ\text{C}$ – $500 \text{ }^\circ\text{C}$ , a slow decomposition of the organic carbonaceous matter took place. Beyond  $500 \text{ }^\circ\text{C}$  the observed mass loss could be mainly assigned to the elimination of heteroatoms, i.e., oxygen and nitrogen atoms. Thus, the highest weight loss was observed for the C-ZN sample with the highest content of heteroatoms ( $\sim 32 \text{ wt.}\%$ )

(see Table 1). The thermal stability of the prepared activated carbons is much better than other biomass-derived carbons reported in the literature [40,41].

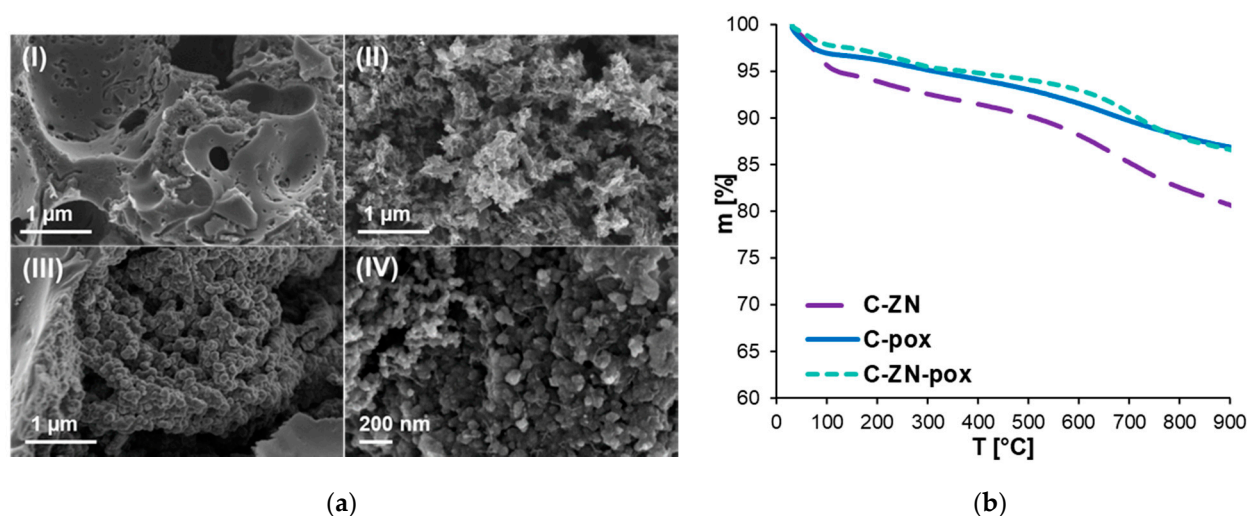


**Figure 1.** (a) SEM images of (I) C-pox, (II) C-ZN-pox, (III,IV) C-ZN; (b) thermogravimetric curves of C-ZN, C-pox and C-ZN-pox.

**Table 1.** Element concentrations in the selected activated carbon samples.

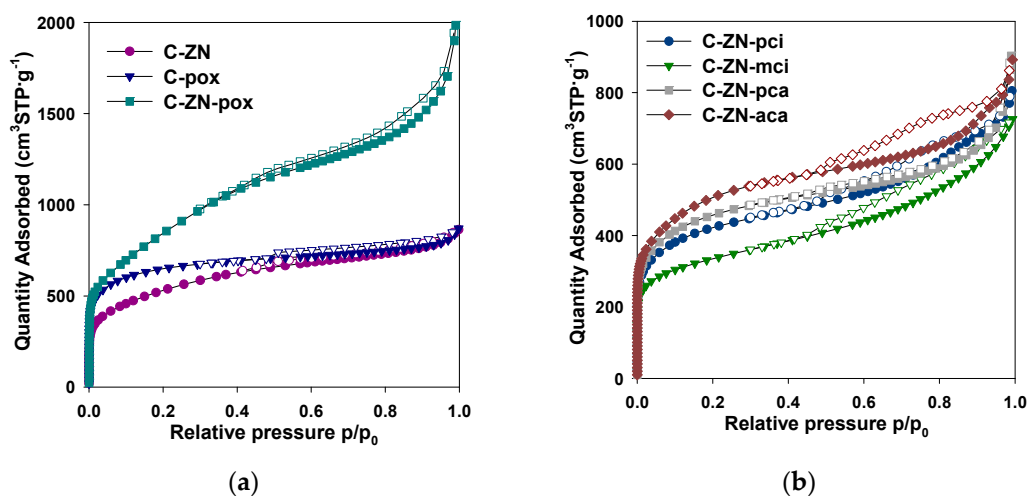
Samples	C (wt.%)	H (wt.%)	N (wt.%)
C-ZN	67.52	2.84	5.60
C-pox	71.02	2.19	1.01
C-ZN-pox	74.20	1.83	5.94

Table 2 summarizes structural parameters determined from low-temperature nitrogen adsorption/desorption isotherms for all prepared samples (shown in Figure 2). The high uptake of nitrogen at low pressure indicates microporous structures, whereas the observed hystereses confirm the presence of mesopores in the obtained carbons. Therefore, the measured nitrogen isotherms are a combination of both types I and IV isotherms according to the IUPAC classification [42]. The presence of different pore sizes in the range of micro- and mesopores is also evidenced by the determined pore size distribution (PSD) functions (Figure 3) calculated in the range of micropores (<2 nm) and small mesopores (from 2 nm to 5 nm). The values of SSA and total pore volume ( $V_t$ ) ranged from 1190 to 3060  $\text{m}^2 \cdot \text{g}^{-1}$  and from 1.12 to 3.07  $\text{cm}^3 \cdot \text{g}^{-1}$ , respectively.

**Table 2.** Structural parameters calculated from low-temperature ( $-196^\circ\text{C}$ ) nitrogen adsorption data for all samples studied.

Sample	SSA <sup>1</sup> ( $\text{m}^2 \cdot \text{g}^{-1}$ )	$V_t$ <sup>2</sup> ( $\text{cm}^3 \cdot \text{g}^{-1}$ )	$V_{\text{ultra}}$ <sup>3</sup> ( $\text{cm}^3 \cdot \text{g}^{-1}$ )	$V_{\text{micro}}$ <sup>4</sup> ( $\text{cm}^3 \cdot \text{g}^{-1}$ )	$V_{\text{meso}}$ <sup>5</sup> ( $\text{cm}^3 \cdot \text{g}^{-1}$ )
C-ZN	1910	1.34	0.13	0.60	0.74
C-pox	2330	1.35	0.21	0.87	0.48
C-ZN-pox	3060	3.07	0.09	0.77	2.30
C-ZN-aca	1832	1.38	0.16	0.61	0.77
C-ZN-pca	1645	1.40	0.11	0.56	0.84
C-ZN-pci	1520	1.25	0.12	0.50	0.75
C-ZN-mci	1190	1.12	0.14	0.38	0.74

<sup>1</sup> SSA—specific surface area, calculated by the Brunauer–Emmett–Teller method. <sup>2</sup>  $V_t$ —total pore (single-point) volume, obtained from the amount of adsorbed nitrogen at  $p/p_0 \approx 0.99$ . <sup>3</sup>  $V_{\text{ultra}}$ —volume of ultramicropores (pores <0.7 nm). <sup>4</sup>  $V_{\text{micro}}$ —volume of micropores (pores <2.0 nm). <sup>5</sup>  $V_{\text{meso}}$ —volume of mesopores—difference between  $V_t$  and  $V_{\text{micro}}$ .



**Figure 2.** (a) Low-temperature nitrogen adsorption-desorption isotherms measured for C-ZN, C-pox and C-ZN-pox; (b) low-temperature nitrogen adsorption-desorption isotherms measured for C-ZN-aca, C-ZN-pca, C-ZN-pci and C-ZN-mci. The filled points refer to adsorption, whereas the open points correspond to desorption processes.

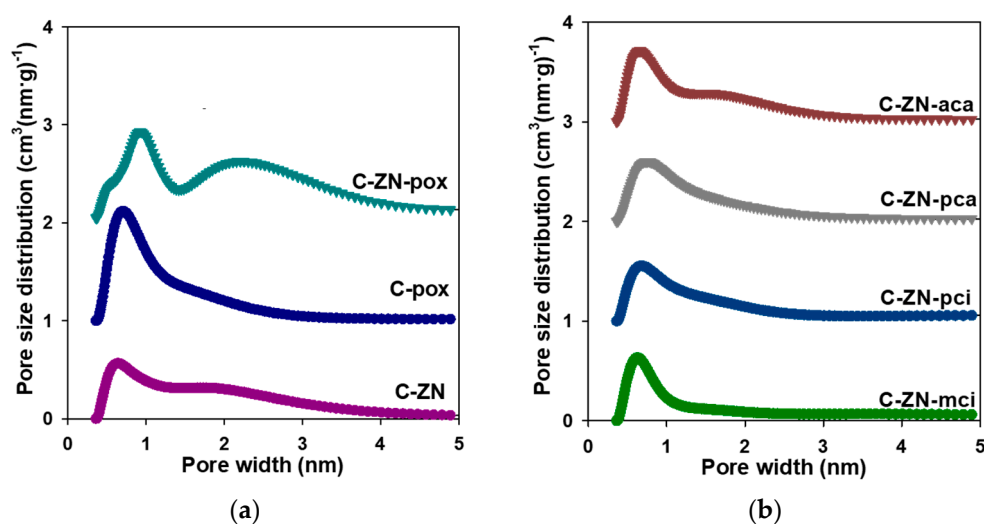


**Figure 3.** (a) Pore size distributions determined for C-ZN, C-pox and C-ZN-pox; (b) pore size distributions determined for C-ZN-aca, C-ZN-pca, C-ZN-pci and C-ZN-mci. For clarity the  $y$ -axis for each subsequent pore size distribution (PSD) curve was shifted upward by  $1 \text{ cm}^3 \cdot (\text{g} \cdot \text{nm})^{-1}$ .

In this work, the influence of various activators on the structural parameters of the resulting carbons is discussed. According to Table 1,  $\text{K}_2\text{C}_2\text{O}_4$  was the most effective agent among other salts (such as  $\text{K}_3\text{C}_6\text{H}_5\text{O}_7$ ,  $\text{MgC}_6\text{H}_6\text{O}_7$ ,  $\text{K}_2\text{CO}_3$  and  $(\text{NH}_4)_2\text{CO}_3$ ) used for activation of the TA-derived carbons. Using  $\text{K}_2\text{C}_2\text{O}_4$  together with the eutectic  $\text{ZnCl}_2/\text{NaCl}$  mixture resulted in obtaining a high porosity carbon (C-ZN-pox), as evidenced by a very high SSA of  $3060 \text{ m}^2 \cdot \text{g}^{-1}$ . Its micro-mesoporous structure featured a large volume of small mesopores (up to  $\sim 4 \text{ nm}$ ), yielding high overall mesoporosity of about 75%. The reference sample C-pox, prepared analogously to C-ZN-pox except for the addition of the eutectic salt of chlorides, exhibited a smaller amount of mesopores, which contributed to its lower SSA ( $2330 \text{ m}^2 \cdot \text{g}^{-1}$ ). However, this sample featured the largest volume of micropores of  $0.87 \text{ cm}^3 \cdot \text{g}^{-1}$ , including a volume of ultramicropores of  $0.21 \text{ cm}^3 \cdot \text{g}^{-1}$ , among all the samples studied. It appears that both activators  $\text{K}_2\text{C}_2\text{O}_4$  and  $\text{ZnCl}_2$  are needed in order to develop high porosity in the TA-derived carbons with SSAs exceeding  $3000 \text{ m}^2 \cdot \text{g}^{-1}$ , which is attributed to a synergetic effect of salt-templating and chemical activation using both inorganic and organic salts [5,43]. Overall, the presence of  $\text{NaCl}$  and  $\text{ZnCl}_2$  salts in the

synthesis generated micropores and small mesopores (between 2 and 5 nm), whereas the addition of potassium oxalate provided a large volume of micropores in the final carbons.

All the salts used in this paper acted as templates during the ball milling of carbon precursors.  $\text{ZnCl}_2$  and the additional potassium and ammonium salts also served as activators because they reacted with the carbon precursors upon reaching high temperatures during the one-step carbonization and activation. The templating salt, NaCl, and the residuals of other salts were simply removed by post-synthetic washing. Overall, the facile mechanochemical strategy resulted in the formation of a vast number of small pores, usually in the range of micropores and tiny mesopores (2–4 nm) in the carbon structures. The samples obtained using citrates and carbonates as activating agents featured lower values of the structural parameters SSA and  $V_t$  as compared to those of C-ZN-pox, C-pox and even C-ZN, which can be linked to the different condensation mechanisms during the thermal treatment process.

## 2.2. $\text{H}_2$ and $\text{CO}_2$ Adsorption

Carbon dioxide and hydrogen adsorption isotherms were measured for the selected samples (C-ZN, C-pox and C-ZN-pox) to further characterize their structures and adsorption properties (Figure 4). The  $\text{CO}_2$  and  $\text{H}_2$  adsorption capacities of the carbons are summarized in Table 3. As expected, C-pox adsorbed the highest amount of  $\text{CO}_2$ — $6.4 \text{ mmol}\cdot\text{g}^{-1}$  at  $0^\circ\text{C}$  and 1 bar—because of its well-developed microporosity with a large volume of ultramicropores ( $V_{\text{ultra}} = 0.21 \text{ cm}^3\cdot\text{g}^{-1}$ ). Ultramicropores provide a strong adsorption affinity toward  $\text{CO}_2$  molecules due to the overlapping force fields of the opposite pore walls, leading to the strong adsorption of  $\text{CO}_2$  molecules. Hence, the samples with similar total pore volume (C-ZN) and even the one with the highest SSA (C-ZN-pox) exhibited lower  $\text{CO}_2$  uptakes ( $4.4$  and  $4.7 \text{ mmol}\cdot\text{g}^{-1}$ , respectively) due to lower volume of ultramicropores in their structures ( $0.13$  and  $0.09 \text{ cm}^3\cdot\text{g}^{-1}$ , respectively). These results clearly confirm that ultramicropores determine high  $\text{CO}_2$  uptake at ambient pressure [44]. Additionally, the prepared carbons contain nitrogen, originating from the urea used in the synthesis [12,21], which undoubtedly had an influence on their excellent  $\text{CO}_2$  adsorption properties, since  $\text{CO}_2$  molecules are attracted by N species via acid–base interactions [45–47]. In the case of hydrogen adsorption, the highest values of adsorption of  $\text{H}_2$ , namely  $13.2 \text{ mmol}\cdot\text{g}^{-1}$  and  $12.9 \text{ mmol}\cdot\text{g}^{-1}$  at  $-196^\circ\text{C}$  and 1 bar, were observed for C-ZN-pox and C-pox carbons, respectively, which also showed the largest values of SSA.

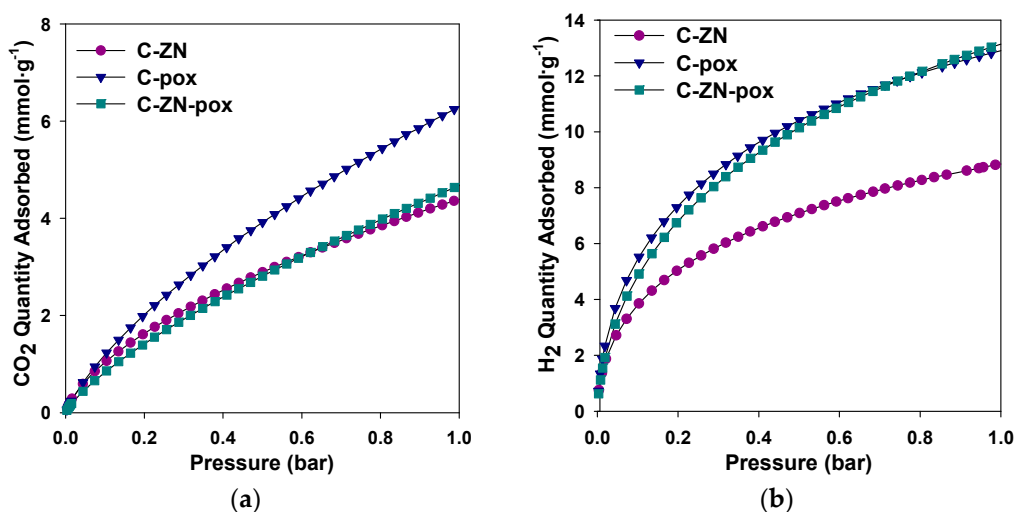


**Figure 4.** (a)  $\text{CO}_2$  adsorption isotherms measured for the selected carbons at  $0^\circ\text{C}$ ; (b)  $\text{H}_2$  adsorption isotherms measured for the selected carbons at  $-196^\circ\text{C}$ .

**Table 3.** Carbon dioxide and hydrogen uptakes for the selected carbon samples.

Samples	CO <sub>2</sub> (mmol·g <sup>-1</sup> ) 0 °C, 1 bar	H <sub>2</sub> (mmol·g <sup>-1</sup> ) −196 °C, 1 bar
C-ZN	4.4	8.9
C-pox	6.4	12.9
C-ZN-pox	4.7	13.2

Hydrogen and carbon dioxide adsorption measurements provide more comprehensive characterization of the synthesized materials and were consistent with the results obtained from the nitrogen adsorption isotherms. The simple and relatively fast mechanochemical synthesis, followed by one-step carbonization and activation presented here afforded highly porous sustainable carbons that can be used for a variety of applications such as adsorption or catalysis. For instance, the calculated structural parameters for C-ZN-pox, which revealed a high micro-mesoporous porosity, suitable for the adsorption of other gases and vapors, including volatile organic compounds as well as various pollutants from contaminated water.

Table 4 comprises the obtained results, along with reports from the literature. So far, the materials obtained in this paper belong among the most porous biomass-derived activated carbons prepared (with the highest SSAs) via the ball milling strategy [12,18,21,48,49].

**Table 4.** Comparison of biomass-derived activated carbons obtained via mechanochemically-assisted syntheses.

Sample	Carbon Source/Activator	SSA [m <sup>2</sup> ·g <sup>-1</sup> ]	Application	Ref.
C-ZN	Tannic acid/ZnCl <sub>2</sub>	1910	CO <sub>2</sub> adsorption (4.4 mmol·g <sup>-1</sup> at 0 °C and 1 bar) H <sub>2</sub> adsorption (8.9 mmol·g <sup>-1</sup> at −196 °C and 1 bar)	This work
C-pox	Tannic acid/K <sub>2</sub> C <sub>2</sub> O <sub>4</sub>	2330	CO <sub>2</sub> adsorption (6.4 mmol·g <sup>-1</sup> at 0 °C and 1 bar) H <sub>2</sub> adsorption (12.9 mmol·g <sup>-1</sup> at −196 °C and 1 bar)	This work
C-ZN-pox	Tannic acid/ZnCl <sub>2</sub> , K <sub>2</sub> C <sub>2</sub> O <sub>4</sub>	3060	CO <sub>2</sub> adsorption (4.7 mmol·g <sup>-1</sup> at 0 °C and 1 bar) H <sub>2</sub> adsorption (13.2 mmol·g <sup>-1</sup> at −196 °C and 1 bar)	This work
LUPC	Lignin/K <sub>2</sub> CO <sub>3</sub>	3199	Li-S batteries	[12]
WWUPC	Wood waste/K <sub>2</sub> CO <sub>3</sub>	2988	Li-S batteries	[12]
TUPC	Tannic acid/K <sub>2</sub> CO <sub>3</sub>	2873	Li-S batteries	[12]
LD2600P	Lignin/KOH	2224	CO <sub>2</sub> adsorption (4.5 mmol·g <sup>-1</sup> at 25 °C and 1 bar)	[48]
NDAB3-500	<i>Arundo donax</i> and chitosan/ZnCl <sub>2</sub>	1863	CO <sub>2</sub> adsorption (2.1 mmol·g <sup>-1</sup> at 25 °C and 1 bar)	[18]
HSAC-MCS-900-9	Coconut shel/-	1771	Li-S batteries and creatinine adsorption	[49]
TA_0	Tannic acid/ZnCl <sub>2</sub>	1570	Supercapacitors	[21]
SD2650P	Sawdust/KOH	1313	CO <sub>2</sub> adsorption (5.8 mmol·g <sup>-1</sup> at 25 °C and 1 bar)	[48]

### 3. Materials and Methods

#### 3.1. Starting Materials

Sodium chloride (99.9%) and zinc chloride, used to prepare the eutectic mixture, were supplied by POCH S.A. Tannic acid and urea (99.9%), i.e., carbon and nitrogen precursors, were provided by the CarboSynth and Lach-Ner, respectively. Activators, namely potassium oxalate (99.5%), potassium carbonate (99%) and ammonium carbonate, were purchased from CHEMPUR (Piekary Śląskie, Poland), whereas potassium citrate

(99%) was from Sigma-Aldrich (Munich, Germany) and magnesium citrate (95%) was from Fluka (Munich, Germany). All chemicals were used without further purification.

### 3.2. Synthesis Procedure

To prepare highly porous carbons we employed and modified the facile mechanochemical concept for the synthesis of porous carbons from tannic acid (TA) and urea (U) reported by Tiruye et al. [21]. Herein, we used additional/different salts to develop the porosity of the resulting activated carbons. In brief, a eutectic salt was prepared by 5 min milling of  $\text{ZnCl}_2$  and  $\text{NaCl}$  with a 29% mole fraction of  $\text{NaCl}$  in Planetary Mono Mill Pulverisette classic line ball milling machine (Fritsch, Bahnhofstraße, Germany). Then, TA and U were added, together with one of the following activators— $\text{K}_2\text{C}_2\text{O}_4$ ,  $\text{K}_3\text{C}_6\text{H}_5\text{O}_7$ ,  $\text{MgC}_6\text{H}_6\text{O}_7$ ,  $\text{K}_2\text{CO}_3$  or  $(\text{NH}_4)_2\text{CO}_3$ —and small amount of deionized water (adjusted to obtain a semi-solid homogenous paste) and mixed in the ball miller for 1 h at 500 rpm using a molar ratio of 13:1 (U:TA). The mass ratio of precursors (TA + U) to the eutectic salt ( $\text{ZnCl}_2/\text{NaCl}$ ) was 1:3, whereas the mass ratio of the additional salt to the eutectic salt was 1:1. The as-prepared paste was activated at 800 °C in nitrogen atmosphere for 1 h. Next, the resulting solid was purified in 1 M HCl and stirred with a magnetic stirrer overnight to remove residues from pores. Finally, it was washed several times with deionized water, filtered and dried overnight in an oven at 80 °C. The as-prepared carbons are denoted as C-ZN- $x$ , where ZN refers to the eutectic salt and  $x$  represents the activator used—pox (potassium oxalate,  $\text{K}_2\text{C}_2\text{O}_4$ ), aca (ammonium carbonate,  $(\text{NH}_4)_2\text{CO}_3$ ), pca (potassium carbonate,  $\text{K}_2\text{CO}_3$ ), pci (potassium citrate,  $\text{K}_3\text{C}_6\text{H}_5\text{O}_7$ ) or mci (magnesium citrate,  $\text{MgC}_6\text{H}_6\text{O}_7$ ). Additionally, C-pox was obtained using the same recipe as C-ZN-pox, except for the addition of ZN. Figure 5 shows a schematic representation of the synthesis procedure.

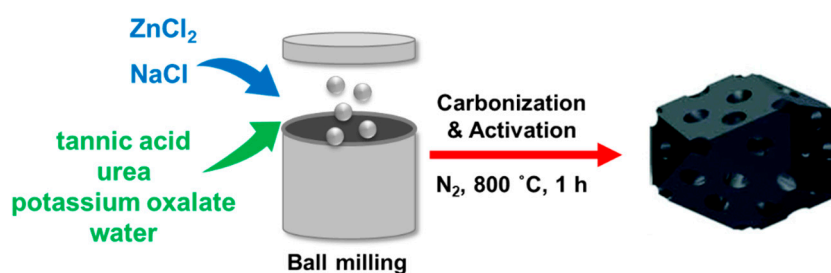


**Figure 5.** Scheme illustrating the synthesis of tannic acid-derived activated carbons.

### 3.3. Measurements and Calculations

The SEM images were performed by using a scanning electron microscope LEO 1530 manufactured by Zeiss (Oberkochen, Germany) at 2 kV acceleration voltage. The thermal stability of activated carbons was examined by thermogravimetric analysis performed on Setaram Labsys TG (Caluire-et-Cuire, France) under the following operational conditions: heating rate  $5\text{ °C}\cdot\text{min}^{-1}$ , nitrogen atmosphere, temperature range of 30 °C–900 °C. An elemental analysis to assess C, H and N wt.% content was performed using a Vario EL Cube apparatus (Elementar, Langensfeld, Germany). Nitrogen adsorption isotherms were measured at  $-196\text{ °C}$  using a ASAP 2020 volumetric analyzer manufactured by Micromeritics Instrument Corp. (Norcross, GA, USA). Hydrogen and carbon dioxide isotherms were measured at  $-196\text{ °C}$  and  $0\text{ °C}$ , respectively. All samples were outgassed for 2 h at 200 °C prior to the adsorption measurements. Specific surface area (SSA) was calculated from low temperature nitrogen adsorption data in a relative pressure range of  $0.05 < p/p_0 < 0.2$  using the Brunauer–Emmett–Teller method [50]. Total pore volume ( $V_t$ ) was calculated using the volume of liquid nitrogen adsorbed at a relative pressure  $\sim 0.99$ . Pore size distribution (PSD) and micropore volume ( $V_{\text{micro}}$ ) were calculated from low-temperature nitrogen adsorption data using the non-local density functional theory (2D-NLDFT) method for carbons with slit-shaped pores, taking into account the energetic heterogeneity and geometrical corrugation of the surface [51,52]. The calculations were

performed using the numerical program SAIEUS. The mesopore volume ( $V_{\text{meso}}$ ) was calculated as the difference between  $V_t$  and  $V_{\text{micro}}$ .

#### 4. Conclusions

This work demonstrates the mechanochemical synthesis of N-doped activated carbons from sustainable precursors tannic acid and urea using a combined salt-templating strategy and chemical activation. This mechanochemical approach is environmentally friendly due to the reduction of both synthesis time and solvent usage compared to more traditional wet chemistry. Moreover, the biomass-derived compound tannic acid is employed as a carbon source and sustainable inorganic and organic salts are used as templates and activators. To show the influence of different activators on the resulting carbons, a series of organic and inorganic salts was examined— $\text{K}_2\text{C}_2\text{O}_4$ ,  $\text{K}_3\text{C}_6\text{H}_5\text{O}_7$ ,  $\text{MgC}_6\text{H}_6\text{O}_7$ ,  $\text{K}_2\text{CO}_3$  and  $(\text{NH}_4)_2\text{CO}_3$ . Their physicochemical characterization revealed that the activators used had a significant impact on the morphology, thermal stability, porosity and adsorption properties of the obtained carbons. In particular, simultaneous activation by zinc chloride and potassium oxalate led to an outstanding porosity in the resulting carbon (SSA of  $3060 \text{ m}^2 \cdot \text{g}^{-1}$  and  $V_t$  of  $3.07 \text{ cm}^3 \cdot \text{g}^{-1}$ ) and superior gas adsorption properties ( $\text{H}_2$  and  $\text{CO}_2$  uptakes at ambient pressure,  $-196$  and  $0$  °C, equal to  $13.2 \text{ mmol} \cdot \text{g}^{-1}$  and  $4.7 \text{ mmol} \cdot \text{g}^{-1}$ , respectively). The presented mechanochemical salt-templating method complies with the principles of Green Chemistry and is a promising method for the large-scale production of highly porous activated carbons. It should be emphasized that although the used mechanochemical route is green, a purification step involving washing with HCl (an acidifying reagent for the environment) is often needed, as in this case. Moreover, zinc-based salts are also not recommended as activation agents, due to the related environmental problems. In our approach, the  $\text{ZnCl}_2$  content in the synthesis of most activated carbons was about ~36 wt.%, except for the reference sample, C-ZN (~63 wt.%). Given the above, we also prepared activated carbon without the addition of Zn-containing salts and therefore without the necessity of using HCl solution for washing. It was revealed that using only three sustainable carbon-rich reagents—tannic acid, urea and potassium oxalate—afforded a micro-mesoporous carbon with a high SSA of  $2330 \text{ m}^2 \cdot \text{g}^{-1}$  and a  $\text{CO}_2$  uptake capacity as high as  $6.4 \text{ mmol} \cdot \text{g}^{-1}$  at 1 bar, which makes it an attractive sorbent for real applications.

**Author Contributions:** Conceptualization, S.G. and B.S.; methodology, S.G.; validation, S.G., B.S. and J.C.; formal analysis, B.S., J.C. and M.J.; investigation, S.G.; resources, B.S. and J.C.; writing—original draft preparation, S.G. and B.S.; writing—review and editing, J.C. and M.J.; visualization S.G.; supervision, B.S., J.C. and M.J.; project administration J.C. and M.J. All authors have read and agreed to the published version of the manuscript.

**Funding:** This research received no external funding.

**Data Availability Statement:** Data are available from the authors on request.

**Conflicts of Interest:** The authors declare no conflict of interest.

**Sample Availability:** Carbon samples are available from the authors.

#### References

1. Ali, I.; Asim, M.; Khan, T.A. Low cost adsorbents for the removal of organic pollutants from wastewater. *J. Environ. Manag.* **2012**, *113*, 170–183. [[CrossRef](#)]
2. Dissanayake, P.D.; You, S.; Igalavithana, A.D.; Xia, Y.; Bhatnagar, A.; Gupta, S.; Kua, H.W.; Kim, S.; Kwon, J.H.; Tsang, D.C.W.; et al. Biochar-based adsorbents for carbon dioxide capture: A critical review. *Renew. Sustain. Energy Rev.* **2020**, *119*, 109582. [[CrossRef](#)]
3. Wang, J.; Zhang, X.; Li, Z.; Ma, Y.; Ma, L. Recent progress of biomass-derived carbon materials for supercapacitors. *J. Power Sources* **2020**, *451*, 227794. [[CrossRef](#)]
4. Pampel, J.; Denton, C.; Fellingner, T.P. Glucose derived ionothermal carbons with tailor-made porosity. *Carbon* **2016**, *107*, 288–296. [[CrossRef](#)]
5. Diez, N.; Ferrero, G.A.; Sevilla, M.; Fuertes, A.B. A sustainable approach to hierarchically porous carbons from tannic acid and their utilization in supercapacitive energy storage systems. *J. Mater. Chem. A* **2019**, *7*, 14280–14290. [[CrossRef](#)]

6. Tan, D.; García, F. Main group mechanochemistry: From curiosity to established protocols. *Chem. Soc. Rev.* **2019**, *48*, 2274–2292. [[CrossRef](#)] [[PubMed](#)]
7. Rightmire, N.R.; Hanusa, T.P. Advances in organometallic synthesis with mechanochemical methods. *Dalton Trans.* **2016**, *45*, 2352–2362. [[CrossRef](#)] [[PubMed](#)]
8. Horie, K.; Barón, M.; Fox, R.B.; He, J.; Hess, M.; Kahovec, J.; Kitayama, T.; Kubisa, P.; Maréchal, E.; Mormann, W.; et al. Definitions of terms relating to reactions of polymers and to functional polymeric materials (IUPAC Recommendations 2003). *Pure Appl. Chem.* **2004**, *76*, 889–906. [[CrossRef](#)]
9. Takacs, L. Two important periods in the history of mechanochemistry. *J. Mater. Sci.* **2018**, *53*, 13324–13330. [[CrossRef](#)]
10. Takacs, L. The historical development of mechanochemistry. *Chem. Soc. Rev.* **2013**, *42*, 7649–7659. [[CrossRef](#)]
11. Boldyreva, E. Mechanochemistry of inorganic and organic systems: What is similar, what is different? *Chem. Soc. Rev.* **2013**, *42*, 7719–7738. [[CrossRef](#)]
12. Schneidermann, C.; Kensy, C.; Otto, P.; Oswald, S.; Giebeler, L.; Leistenschneider, D.; Grätz, S.; Dörfler, S.; Kaskel, S.; Borchardt, L. Nitrogen-doped biomass-derived carbon formed by mechanochemical synthesis for lithium–sulfur batteries. *ChemSusChem* **2019**, *12*, 310–319. [[CrossRef](#)]
13. Schneidermann, C.; Jäckel, N.; Oswald, S.; Giebeler, L.; Presser, V.; Borchardt, L. Solvent-free mechanochemical synthesis of nitrogen-doped nanoporous carbon for electrochemical energy storage. *ChemSusChem* **2017**, *10*, 2416–2424. [[CrossRef](#)] [[PubMed](#)]
14. Tzvetkov, G.; Mihaylova, S.; Stoitchkova, K.; Tzvetkov, P.; Spassov, T. Mechanochemical and chemical activation of lignocellulosic material to prepare powdered activated carbons for adsorption applications. *Powder Technol.* **2016**, *299*, 41–50. [[CrossRef](#)]
15. Cai, C.; Fu, N.; Zhou, Z.; Wu, M.; Yang, Z.; Liu, R. Mechanochemical synthesis of tannic acid-Fe coordination compound and its derived porous carbon for CO<sub>2</sub> adsorption. *Energy Fuels* **2018**, *32*, 10779–10785. [[CrossRef](#)]
16. Qi, J.; Zhang, W.; Xu, L. Solvent-free mechanochemical preparation of hierarchically porous carbon for supercapacitor and oxygen reduction reaction. *Chem. Eur. J.* **2018**, *24*, 18097–18105. [[CrossRef](#)]
17. Rajendiran, R.; Nallal, M.; Park, K.H.; Li, O.L.; Kim, H.J.; Prabakar, K. Mechanochemical assisted synthesis of heteroatoms inherited highly porous carbon from biomass for electrochemical capacitor and oxygen reduction reaction electrocatalysis. *Electrochim. Acta* **2019**, *317*, 1–9. [[CrossRef](#)]
18. Singh, G.; Kim, I.Y.; Lakhi, K.S.; Joseph, S.; Srivastava, P.; Naidu, R.; Vinu, A. Heteroatom functionalized activated porous biocarbons and their excellent performance for CO<sub>2</sub> capture at high pressure. *J. Mater. Chem. A* **2017**, *5*, 21196–21204. [[CrossRef](#)]
19. Schneidermann, C.; Otto, P.; Leistenschneider, D.; Grätz, S.; Eßbach, C.; Borchardt, L. Upcycling of polyurethane waste by mechanochemistry: Synthesis of N-doped porous carbon materials for supercapacitor applications. *Beilstein J. Nanotechnol.* **2019**, *10*, 1618–1627. [[CrossRef](#)] [[PubMed](#)]
20. Leistenschneider, D.; Wegner, K.; Eßbach, C.; Sander, M.; Schneidermann, C.; Borchardt, L. Tailoring the porosity of a mesoporous carbon by a solvent-free mechanochemical approach. *Carbon* **2019**, *147*, 43–50. [[CrossRef](#)]
21. Tiruye, G.A.; Muñoz-Torrero, D.; Berthold, T.; Palma, J.; Antonietti, M.; Fechler, N.; Marcilla, R. Functional porous carbon nanospheres from sustainable precursors for high performance supercapacitors. *J. Mater. Chem. A* **2017**, *5*, 16263–16272. [[CrossRef](#)]
22. Zhang, W.; Qi, J.; Bai, P.; Wang, H.; Xu, L. High-level nitrogen-doped, micro/mesoporous carbon as an efficient metal-free electrocatalyst for the oxygen reduction reaction: Optimizing the reaction surface area by a solvent-free mechanochemical method. *New J. Chem.* **2019**, *43*, 10878–10886. [[CrossRef](#)]
23. Casco, M.E.; Kirchhoff, S.; Leistenschneider, D.; Rauche, M.; Brunner, E.; Borchardt, L. Mechanochemical synthesis of N-doped porous carbon on room temperature. *Nanoscale* **2019**, *11*, 4712–4718. [[CrossRef](#)] [[PubMed](#)]
24. Tan, X.-F.; Liu, S.-B.; Liu, Y.-G.; Gu, Y.-L.; Zeng, G.-M.; Hu, X.-J.; Wang, X.; Liu, S.-H.; Jiang, L.-H. Biochar as potential sustainable precursors for activated carbon production: Multiple applications in environmental protection and energy storage. *Bioresour. Technol.* **2017**, *227*, 359–372. [[CrossRef](#)]
25. Danish, M.; Ahmad, T. A review on utilization of wood biomass as a sustainable precursor for activated carbon production and application. *Renew. Sustain. Energ. Rev.* **2018**, *87*, 1–21. [[CrossRef](#)]
26. Wang, Z.; Shen, D.; Wu, C.; Gu, S. State-of-the-art on the production and application of carbon nanomaterials from biomass. *Green Chem.* **2018**, *20*, 5031–5057. [[CrossRef](#)]
27. Deng, J.; Li, M.; Wang, Y. Biomass-derived carbon: Synthesis and applications in energy storage and conversion. *Green Chem.* **2016**, *18*, 4824–4854. [[CrossRef](#)]
28. Nowicki, P.; Kazmierczak, J.; Pietrzak, R. Comparison of physicochemical and sorption properties of activated carbons prepared by physical and chemical activation of cherry stones. *Powder Technol.* **2015**, *269*, 312–319. [[CrossRef](#)]
29. Pórolniczak, P.; Nowicki, P.; Wasíński, K.; Pietrzak, R.; Walkowiak, M. Biomass-derived hierarchical carbon as sulfur cathode stabilizing agent for lithium-sulfur batteries. *Solid State Ion.* **2016**, *297*, 59–63. [[CrossRef](#)]
30. Nowicki, P.; Pietrzak, R. Carbonaceous adsorbents prepared by physical activation of pine sawdust and their application for removal of NO<sub>2</sub> in dry and wet conditions. *Bioresour. Technol.* **2010**, *101*, 5802–5807. [[CrossRef](#)] [[PubMed](#)]
31. Nowicki, P.; Kazmierczak-Razna, J.; Pietrzak, R. Physicochemical and adsorption properties of carbonaceous sorbents prepared by activation of tropical fruit skins with potassium carbonate. *Mater. Des.* **2016**, *90*, 579–585. [[CrossRef](#)]
32. Fraga-Corral, M.; García-Oliveira, P.; Pereira, A.G.; Lourenço-Lopes, C.; Jimenez-Lopez, C.; Prieto, M.A.; Simal-Gandara, J. Technological application of tannin-based extracts. *Molecules* **2020**, *25*, 614. [[CrossRef](#)]

33. Pizzi, A. Tannins: Prospectives and actual industrial applications. *Biomolecules* **2019**, *9*, 344. [[CrossRef](#)]
34. Braghiroli, F.L.; Fierro, V.; Izquierdo, M.T.; Parmentier, J.; Pizzi, A.; Celzard, A. Nitrogen-doped carbon materials produced from hydrothermally treated tannin. *Carbon* **2012**, *50*, 5411–5420. [[CrossRef](#)]
35. Yao, Y.; Yu, M.; Yin, H.; Wei, F.; Zhang, J.; Hu, H.; Wang, S. Tannic acid-Fe coordination derived Fe/N-doped carbon hybrids for catalytic oxidation processes. *Appl. Surf. Sci.* **2019**, *489*, 44–54. [[CrossRef](#)]
36. Ruiz, B.; Ruisánchez, E.; Gil, R.R.; Ferrera-Lorenzo, N.; Lozano, M.S.; Fuente, E. Sustainable porous carbons from lignocellulosic wastes obtained from the extraction of tannins. *Microporous Mesoporous Mater.* **2015**, *209*, 23–29. [[CrossRef](#)]
37. Sanchez-Sanchez, A.; Izquierdo, M.T.; Medjahdi, G.; Ghanbaja, J.; Celzard, A.; Fierro, V. Ordered mesoporous carbons obtained by soft-templating of tannin in mild conditions. *Microporous Mesoporous Mater.* **2018**, *270*, 127–139. [[CrossRef](#)]
38. Nelson, K.M.; Mahurin, S.M.; Mayes, R.T.; Williamson, B.; Teague, C.M.; Binder, A.J.; Baggetto, L.; Veith, G.M.; Dai, S. Preparation and CO<sub>2</sub> adsorption properties of soft-templated mesoporous carbons derived from chestnut tannin precursors. *Microporous Mesoporous Mater.* **2016**, *222*, 94–103. [[CrossRef](#)]
39. Sanchez-Sanchez, A.; Izquierdo, M.T.; Ghanbaja, J.; Medjahdi, G.; Mathieu, S.; Celzard, A.; Fierro, V. Excellent electrochemical performances of nanocast ordered mesoporous carbons based on tannin-related polyphenols as supercapacitor electrodes. *J. Power Sources* **2017**, *344*, 15–24. [[CrossRef](#)]
40. Bazan, A.; Nowicki, P.; Pórolniczak, P.; Pietrzak, R. Thermal analysis of activated carbon obtained from residue after supercritical extraction of hops. *J. Therm. Anal. Calorim.* **2016**, *125*, 1199–1204. [[CrossRef](#)]
41. Sevilla, M.; Ferrero, G.A.; Fuertes, A.B. One-pot synthesis of biomass-based hierarchical porous carbons with a large porosity development. *Chem. Mater.* **2017**, *29*, 6900–6907. [[CrossRef](#)]
42. Thommes, M.; Kaneko, K.; Neimark, A.; Olivier, J.; Rodriguez-Reinoso, F.; Rouquerol, J.; Sing, K. Physisorption of gases, with special reference to the evaluation of surface area and pore size distribution (IUPAC Technical Report). *Pure Appl. Chem.* **2015**, *87*, 1051–1069. [[CrossRef](#)]
43. Phuriragpitikhon, J.; Ghimire, P.; Jaroniec, M. Tannin-derived micro-mesoporous carbons prepared by one-step activation with potassium oxalate and CO<sub>2</sub>. *J. Colloid Interface Sci.* **2020**, *558*, 55–67. [[CrossRef](#)] [[PubMed](#)]
44. Furmaniak, S.; Kowalczyk, P.; Terzyk, A.P.; Gauden, P.A.; Harris, P.J.F. Synergetic effect of carbon nanopore size and surface oxidation on CO<sub>2</sub> capture from CO<sub>2</sub>/CH<sub>4</sub> mixtures. *J. Colloid Interface Sci.* **2013**, *397*, 144–153. [[CrossRef](#)] [[PubMed](#)]
45. Babu, D.J.; Bruns, M.; Schneider, R.; Gerthsen, D.; Schneider, J.J. Understanding the influence of N-doping on the CO<sub>2</sub> adsorption characteristics in carbon nanomaterials. *J. Phys. Chem. C* **2017**, *121*, 616–626. [[CrossRef](#)]
46. Bandosz, T.J.; Seredych, M.; Rodríguez-Castellon, E.; Cheng, Y.; Daemen, L.L.; Ramírez-Cuesta, A.J. Evidence for CO<sub>2</sub> reactive adsorption on nanoporous S- and N-doped carbon at ambient conditions. *Carbon* **2016**, *96*, 856–863. [[CrossRef](#)]
47. Fulvio, P.F.; Lee, J.S.; Mayes, R.T.; Wang, X.; Mahurin, S.M.; Dai, S. Boron and nitrogen-rich carbons from ionic liquid precursors with tailorable surface properties. *Phys. Chem. Chem. Phys.* **2011**, *13*, 13486–13491. [[CrossRef](#)]
48. Balahmar, N.; Mitchell, A.C.; Mokaya, R. Generalized mechanochemical synthesis of biomass-derived sustainable carbons for high performance CO<sub>2</sub> storage. *Adv. Energy Mater.* **2015**, *5*, 1500867. [[CrossRef](#)]
49. Lin, X.; Liang, Y.; Lu, Z.; Lou, H.; Zhang, X.; Liu, S.; Zheng, B.; Liu, R.; Fu, R.; Wu, D. Mechanochemistry: A green, activation-free and top-down strategy to high-surface-area carbon materials. *ACS Sustain. Chem. Eng.* **2017**, *5*, 8535–8540. [[CrossRef](#)]
50. Braunauer, S.; Emmett, P.H.; Teller, E. Adsorption of gases in multimolecular layers. *J. Am. Chem. Soc.* **1938**, *60*, 309–319. [[CrossRef](#)]
51. Jagiello, J.; Olivier, J.P. 2D-NLDFT adsorption models for carbon slit-shaped pores with surface energetical heterogeneity and geometrical corrugation. *Carbon* **2013**, *55*, 70–80. [[CrossRef](#)]
52. Jagiello, J.; Olivier, J.P. Carbon slit pore model incorporating surface energetical heterogeneity and geometrical corrugation. *Adsorption* **2013**, *19*, 777–783. [[CrossRef](#)]